Int. J. Electrochem. Sci., 15 **(2020)** 10550 – 10569, doi: 10.20964/2020.10.33

International Journal of
ELECTROCHEMICAL
SCIENCE
www.electrochemsci.org

Influences of Duty Cycle and Pulse Frequency on Properties of Ni-SiC Nanocomposites fabricated by Pulse Electrodeposition

Haijun Liu[1], *Hui Wang*[1,*], *Weijun Ying*[1], *Wenqing Liu*[2], *Yong Wang*[2], *Qiang Li*[2]

[1] College of Engineering and Technology, Jiyang College of Zhejiang Agriculture & Forestry University, Zhuji, 311800, China;
[2] College of Mechanical Science and Engineering, Northeast Petroleum University, Daqing 163318, China
[*]E-mail: today2020529@126.com, 20168009@zafu.edu.cn

Received: 30 May 2020 / *Accepted:* 27 July 2020 / *Published:* 31 August 2020

Ni-SiC nanocomposites (NCs) were fabricated using pulse current electrodeposition (PCED) in this article. Influences of PCED frequency and duty cycle on morphology, structure, wear and corrosion behavior of the resulting NCs were thoroughly analyzed using a variety of instrumental techniques such scanning electron and transmission electron microscopies (SEM and TEM, respectively), X-ray diffraction (XRD) as well as wear, corrosion and nanoindentation tests. The results illustrated that the surface of the Ni-SiC NC obtained at the 20% duty cycle contained small Ni grains with smooth, uniform, and fine microstructure. When the coatings were prepared in the 25-50 Hz pulse frequency range, SiC NPs were homogeneously dispersed in the coating, and the resulting NCs were uniform, compact and contained fine grains. Among NCs fabricated at different pulse frequencies and 20% duty cycle, Ni-SiC coatings deposited at 50 Hz showed the highest microhardness value (equal to 911.9 Hv). Wear weight loss of the Ni-SiC NC prepared at 20% duty cycle was only 18.1 mg, which indicates an excellent wear resistance. In addition, EIS of our Ni-SiC NCs deposited at 50 Hz pulse frequency and 20% duty cycle showed the highest impedance, which implies the best corrosion resistance. The result can be applied to the micro precision transmission mechanism for manufacturing various small electric valves and actuators in engine compartments.

Keywords: Ni-SiC NCs; duty cycle; pulse frequency; structure; wear resistance; corrosion resistance

1. INTRODUCTION

Metal-based (MB) nanocomposites (NCs) recently became widely utilized in micro transmission engines mechanism and automobile parts because of their high hardness and shear strength, outstanding corrosion and wear resistance as well as excellent high-temperature oxidation resistance [1-7]. Typically, MBNCs are prepared by electro- or chemical deposition as well as by brush

plating. Electrodeposition (ED) is the fastest and the most straightforward method, also offering low NC fabrication cost [8-12]. Electrodeposition was successfully used to fabricated NCs based on Ni-TiN, Ni-W/SiC, Ni/Ni-TiN, and Ni-CeO_2 [13-16]. Ma *et al.* [13] prepared Ni-Al_2O_3 NCs using A3 steel substrate and a reformative Watt electrolyte and reported that ultrasonic power was critical in determining morphological properties of the resulting NCs. Wasekar *et al.* [14] obtained Ni-W/SiC NCs using pulse current deposition and demonstrated that their morphology and hardness varied as a function of the SiC content. Liu *et al.* [15] electrodeposited bi-layered Ni/Ni-TiN composites containing TiN nanoparticles (NPs) using mild steel as a substrate. Sen *et al.* [16] prepared Ni–CeO_2 NCs by ED technique and observed that the stirring rate affected microhardness, microstructure, and corrosion resistance of the resulting NCs.

Unlike direct current ED, pulse current ED (PCED) is widely used in many industries because it produces more refined matrix grains, increased embedded ceramic contents, and enhanced plating rates. In turn, the resulting matrix grain sizes and ceramic content significantly affect the microhardness of the resulting coating. Size grain of the matrix and the final ceramic component content depend on the PCED parameters (such as pulse frequency and duty cycle). Thus, analysis and understanding of how PCED parameters affect the microstructure and other coating properties is fundamental in needed to produce coatings with the best desired properties.

SiC NPs possess an extraordinary microhardness, high anti-wear and anticorrosion resistances as well as thermal stability [17-19]. Incorporation of SiC NPs into metallic coatings (to enhance their properties) can be realized by PCED. Therefore, this paper reports the fabrication of Ni-SiC NCs by PCED with different duty cycle and pulse frequency parameters to understand how they affect morphology, micro- and phase structures as well as corrosion resistance and wear behavior of the resulting Ni-SiC NC coatings. The result can be applied to the micro precision transmission mechanism for manufacturing various small electric valves and actuators in engine compartments.

2. EXPERIMENT

2.1 Material preparation

The experimental setup used for Ni-SiC NC fabrication consisted of plating and ultrasonic baths, heater, and a pulse current source (see Fig. 1). A composite electrolyte (compositions of which is shown in Table 1) in the plating bath was maintained at 48^{o}C by an AH4-2 heater. To prevent NP agglomeration, a CS-400 type ultrasonicator was used to agitate the plating solution during PECD. A pulse power source (SMD-200) was used as a pulse power source to generate pulses with a certain width (t_{off}) and at specific intervals (t_{on}), which were then used to calculate frequency (f) and duty cycles (r) as shown below:

$$r = \frac{t_{on}}{t_{on} + t_{off}} \quad (1),$$

$$f = \frac{1}{t_{on} + t_{off}} \quad (2).$$

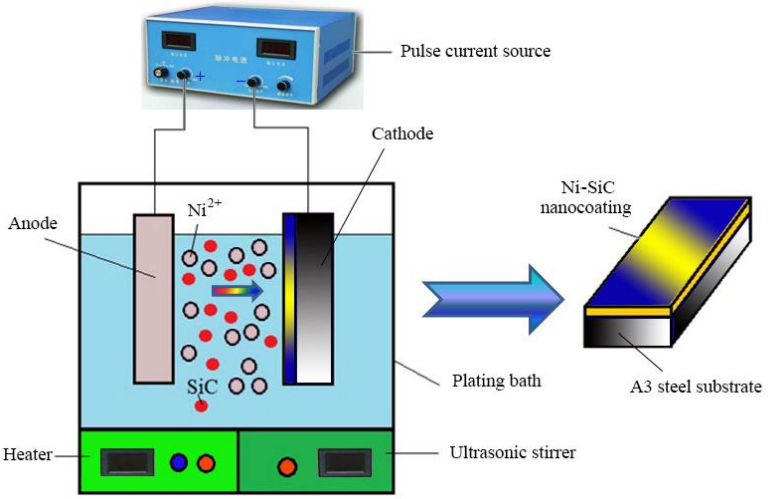

Figure 1. Experimental device for preparing Ni-SiC NCs.

Table 1. Electrolyte composition for depositing Ni-SiC NCs.

Compositions and conditions	Parameters
$NiSO_4 \cdot 6H_2O$ (g/l)	220
$NiCl_2 \cdot H_2O$ (g/l)	60
H_3BO_3 (g/l)	30
SiC nanoparticles (g/l)	15
Plating temperature (°C)	48
pH	4.6
Electroplating time (min)	50

Plating parameters for the Ni-SiC NC deposition on an A3 steel substrate are summarized in Table 2. Electrolyte pH was maintained at 4.6 by 2 M HCl or 2 M NaCl [20]. SiC NPs (with the average size equal to ~35 nm) were purchased from Daqing Tongda Nanotechnology Co. Prior to the PECD, SiC NPs were characterized by TEM (see Fig. 2). Most SiC nanoparticles agglomerated because of their high surface area.

Table 2. Plating parameters for depositing Ni-SiC NCs.

Duty cycle (%)	Pulse width (ms)	Pulse interval (ms)	Pulse frequency (Hz)	Average current density (mA/cm^2)
20	20	80	10	
40	16	24	25	40
80	16	4	50	

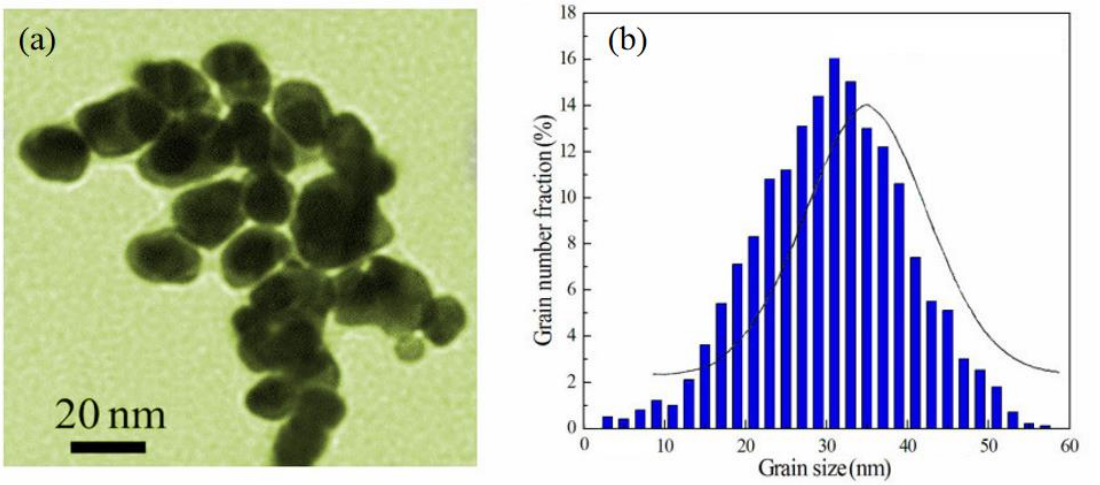

Figure 2. TEM image (a) and size distribution (b) of SiC powders used for preparing Ni-SiC NCs.

2.2 Characterization

Cross-sections and surfaces of the Ni-SiC NCs were analyzed using a scanning electron microscope (SEM, S4800). SiC NP content (denoted as AM-SiC) in the NCs was analyzed by IE-300X energy-dispersive X-ray spectroscope (EDS). Ni-SiC NC microstructural analysis was performed by Tecnai–G2–20–S–Twin transmission electron microscope (TEM). Crystalline phases as a function of the PECD parameters were determined by the D/Max-2400 X-ray diffractometer (XRD) with Cu-Ka radiation. Ni-SiC NC microhardness was tested using diamond Berkovich indenter (model TS-75) using 150 μN and 15 s as an applied load and time, respectively. The wear tests were performed by the MR-H5A instrument using a quenched steel hoop with 65 HRC hardness. Parameters of the test were 180 rpm rotating rate, 120 m wear distance, 10 N applied load, and no lubricants. Weight losses after the wear tests were measured with the 0.1 mg accuracy.

A three-electrode cell and a CS350 electrochemical workstation were utilized to study the Ni-SiC NC corrosion resistance. The Bode and Nyquist curves were recorded using 3.5 wt% NaCl solution as a corrosive solution as well as Ni-SiC NCs, saturated calomel electrode (SCE), and Pt foil as working, reference, and counter electrodes, receptively. Electrochemical impedance spectroscopy (EIS) was performed at an open-circuit voltage (equal to 10 mV) in the 10^{-2}-10^{5} Hz frequency range.

3. RESULTS AND DISCUSSION

3.1 Morphology of the Ni-SiC NCs

3.1.1 SEM observation

The duty cycle significantly affected the surface morphologies of the Ni-SiC NCs according to the SEM micrographs of the materials prepared at different duty cycle values at 50 Hz pulse frequency (see Fig. 3). The surface of the Ni-SiC NC obtained at the 20% duty cycle contained small Ni grains

with smooth, uniform, and fine microstructure (see Fig. 3a). The surface of the Ni-SiC NC obtained at the 40% duty cycle contained rougher and larger Ni grain sizes than the coatings obtained at 20% (see Fig. 3b). Among the NCs prepared at a different duty cycles, Ni-SiC NCs produced at 80% duty cycle possessed the largest Ni grains size (see Fig. 3c). Moreover, the distribution of SiC NPs in this coating was not uniform due to the severe SiC NP agglomeration.

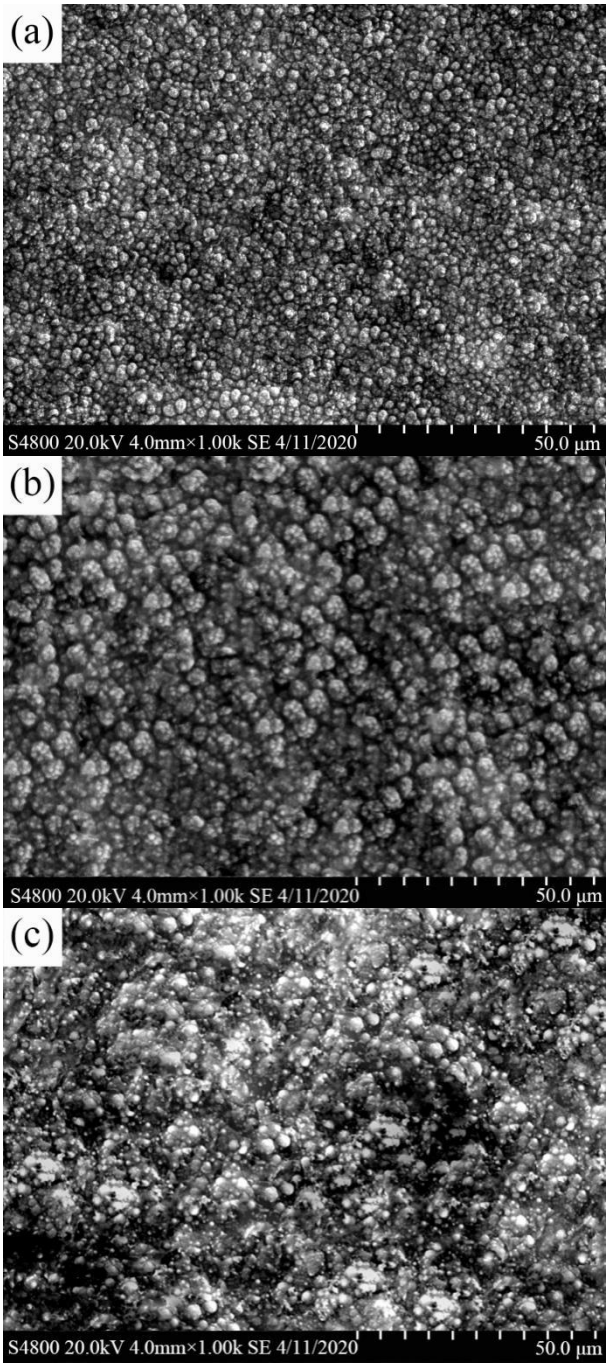

Figure 3. SEM images of Ni-SiC NCs prefabricated with different duty cycles: (a) 20%, (b) 40%, and (c) 80%.

The increase of the Ni grain sizes in the Ni-SiC NCs as a function of the duty cycle can be explained by the following. Typically, the metal grain size increases as the duty cycle increases [21]. At the same pulse frequency, the duty cycle value is proportional to the pulse width. Thus, higher duty cycle values produce wider pulses, which, in our case, increased the amount of Ni^{2+} transport toward the electrode as well as deposition on the cathode. However, the probability of Ni^{2+} ions captured SiC NPs reduced because the concentration of SiC NPs near the cathode decreased. As a result, the content of the SiC NPs in the NC also decreased, diminishing the physical properties of the resulting coating. Because the best coating morphology was obtained at a 20% duty cycle, experiments on the pulse frequency influence on the coating properties were performed using this duty cycle value.

PECD pulse frequency also affected Ni-SiC NC morphology (deposited at the same duty cycle value equal to 20%) (see Fig. 4). At 10 Hz, the resulting Ni-SiC NCs possessed coarse, uneven, and loose-grain microstructure with non-uniform and severely agglomerated SiC NPs (see Fig. 4a). Grain sizes of the Ni-SiC NC obtained at 25 Hz pulse frequency were smaller, and only some particle agglomeration occurred (see Fig. 4b). When the coatings were prepared in the 25-50 Hz pulse frequency range, SiC NPs were homogeneously dispersed in the coating, and the resulting NCs were uniform, compact and contained fine grains (see Fig. 4c).

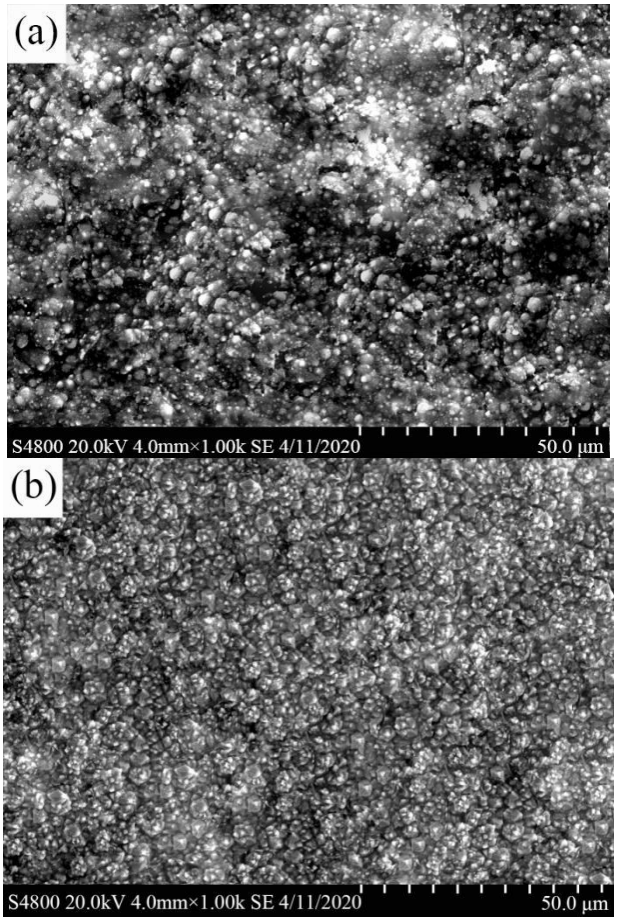

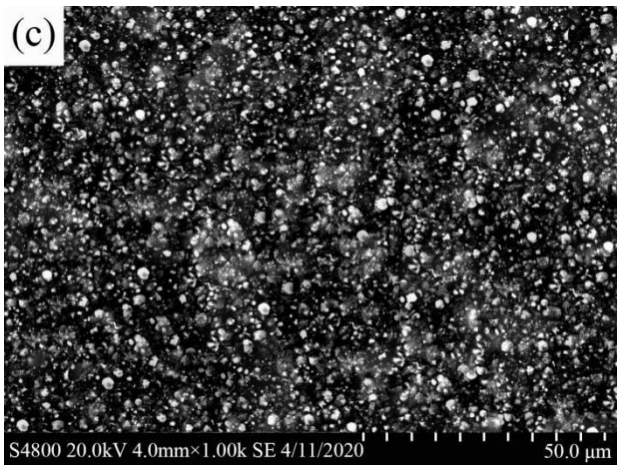

Figure 4. SEM images of Ni-SiC NCs prefabricated with different pulse frequencies: (a) 10 Hz, (b) 25 Hz, and (c) 50 Hz.

Grain size dependency on the pulse frequency can be explained using the formula shown below [22]:

$$J = K\exp(-\frac{\pi\sigma^2 M}{\rho nFRT\eta}) \quad (3)$$

where J and K are the nucleation rate and energy, respectively; σ is the surface free energy between the plating solution and the coating; M is the molecular weight of nickel, ρ is the composite density, n is the number of electrons, F and R are the Faraday and the gas constants, respectively; η is an over-potential, and T is temperature.

Judging by the Equation 3, the over-potential value is most crucial factor affecting the nucleation rate. At high pulse frequencies, an instant over-potential can be generated during just one pulse, enhancing the nucleation. In our case, it would suppress Ni grain growth. Increased pulse frequency also supplies more energy for the adsorption of insoluble NPs [3, 23]. Higher frequencies also led to more SiC NPs being uniformly incorporated into the Ni-SiC NCs simultaneously with Ni^{2+} ions, which results in higher SiC content in the resulting coating. This result could also inhibit the growth of nickel grains. Therefore, as the pulse frequency was increased from 10 to 50 Hz in our PECD experiments, Ni-SiC NC microstructures developed into more uniform, compact, and fine-grained ones.

3.1.2 TEM analysis

TEM of the cross-section of the Ni-SiC sample deposited at 20% duty cycle, and 50 Hz pulse frequency showed abundant and homogeneously distributed SiC NPs in the Ni grains (see Fig. 5). It was also found that the average thickness of this NC was ~70.3 μm.

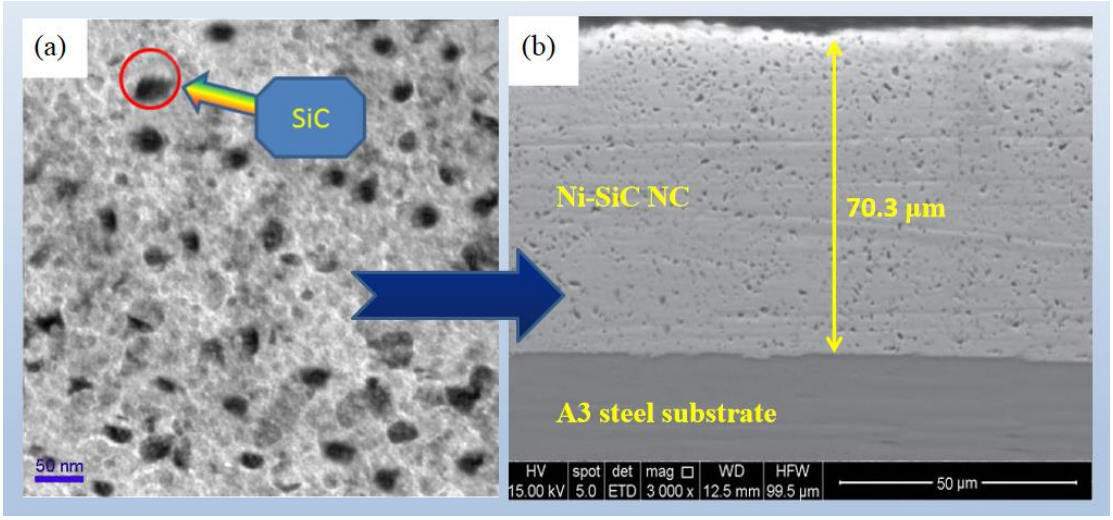

Figure 5. TEM (a) and cross-section (b) images of the as-deposited Ni-SiC NCs prefabricated at 20% duty cycle and 50 Hz pulse frequency.

3.2 SiC NP contents in the nanocomposites

Duty cycle and pulse frequency values also affected SiC NP content: it decreased from 12.5 to 8.2 wt% as the duty cycle value was changed from 20 to 80% (see Fig. 6). Experiments with lower duty cycles (but at the same pulse frequency) were characterized by longer t_{off} . During this time, Ni^{2+} captured numerous SiC NPs, enhancing their incorporation into the composites. The same phenomenon was observed in similar experiments [24]. As duty cycle value increased, the t_{off} became shorter, and the SiC NPs near the cathode could not be replenished in time, resulting in a decrease in the number of SiC NPs captured by Ni^{2+}. Thus, the amount of the deposited SiC NPs decreased.

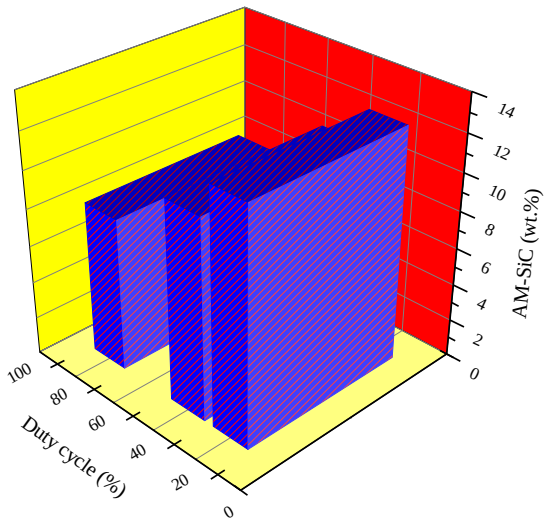

Figure 6. Effect of duty cycle on AM-SiC of SiC NPs in Ni-SiC NCs prefabricated at 50 Hz pulse frequency.

SiC NPs contents in the Ni-SiC NCs increased from 7.6 to 11.4 wt% as the pulse frequency was changed from 10 to 50 Hz (see Fig. 7), which agrees with the literature data [21, 23]. The higher PECD pulse frequencies often lead to increase the over-potential value of Ni^{2+} in the plating solution. Thus, in our system, Ni^{2+} possessed higher energies and adsorbed more of the SiC NPs at higher pulse frequencies. As a result, more SiC NPs were moving towards the cathode under the electrostatic forces, which increased the number of SiC NPs deposited into the coating. At low pulse frequencies, the ability of Ni^{2+} metal particles to adsorb SiC NPs was lower; therefore, only a small number of SiC NPs were delivered to the cathode under the electrostatic force. Therefore, fewer SiC NPs co-deposited into the coating.

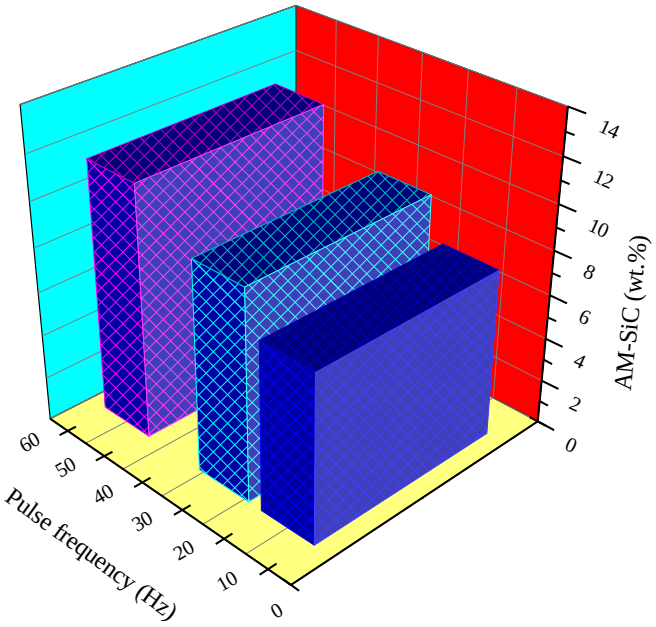

Figure 7. Effect of pulse frequency on AM-SiC of SiC NPs in Ni-SiC NCs prefabricated at 20% duty cycle.

3.3 XRD measurements

XRD patterns of the Ni-SiC demonstrated only weak SiC peaks (see Figs. 8 and 9) because of the overall low SiC content (4-15 times less than that of the Ni). XRD peaks observed at 44.4°, 52.3°, and 76.7° were attributed to the (1 1 1), (2 0 0) and (2 2 0) planes of metallic Ni, respectively. These peaks decreased and became broader as the pulse frequency was increased, and duty cycle value was decreased because of the Ni grain size reduction, the mechanism of which was explained in the previous sections.

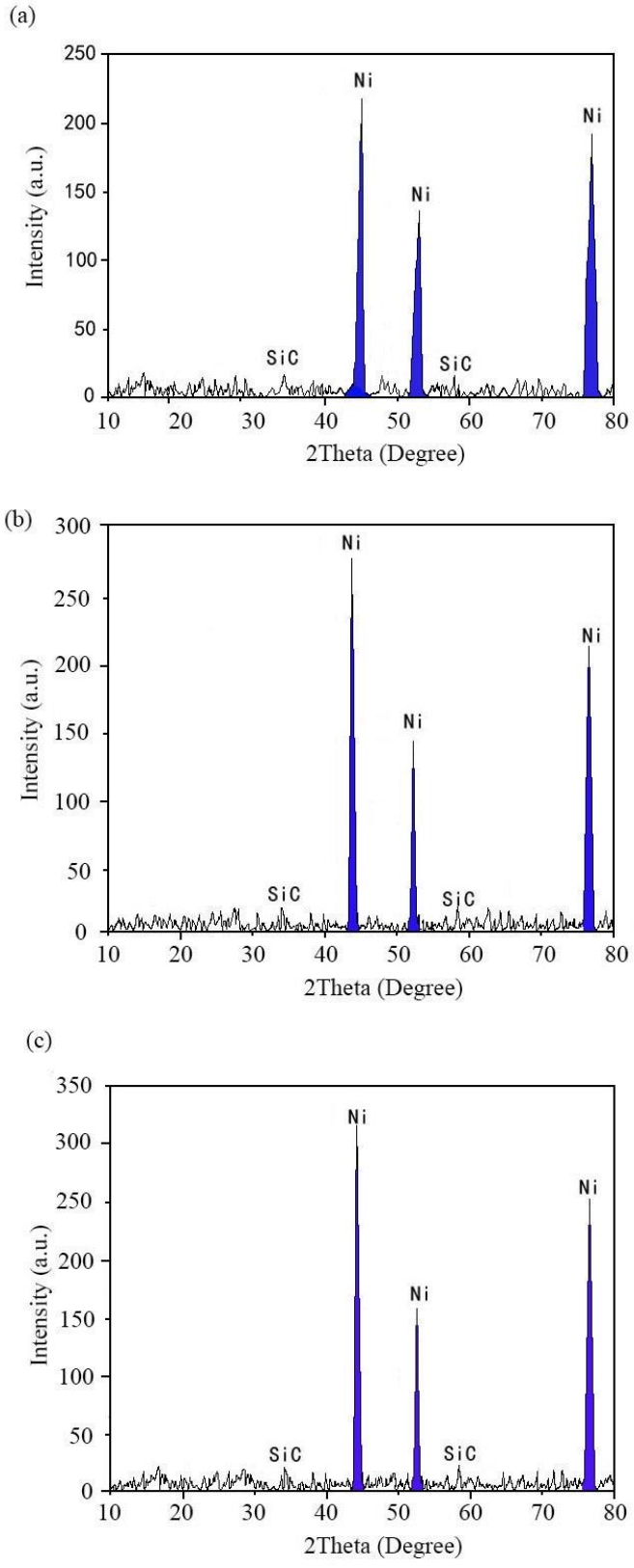

Figure 8. XRD patterns of Ni-SiC NCs prefabricated with different duty cycles: (a) 20%, (b) 40%, and (c) 80%.

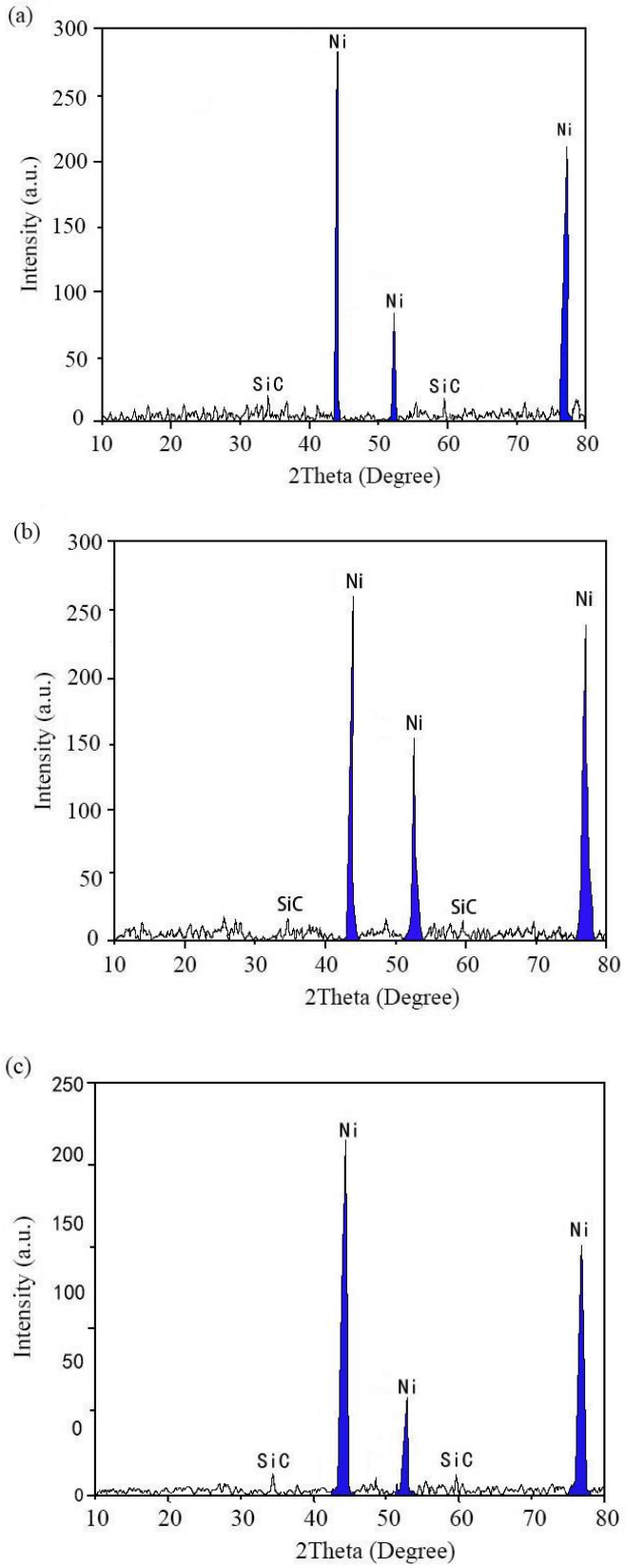

Figure 9. XRD patterns of Ni-SiC NCs prefabricated with different pulse frequencies: (a) 10 Hz, (b) 25 Hz, and (c) 50 Hz.

3.4 Microhardness measurements

Duty cycle value and pules frequency also had an impact on the Ni-SiC NC microhardness (see Figs. 10 and 11). Among Ni-SiC NCs obtained at 20-80% duty cycles (at constant 50 Hz pulse frequency), NCs deposited at 20% duty cycle value demonstrated the highest microhardness equal to 925.4 Hz. Among NCs fabricated at different pulse frequencies and 20% duty cycle, Ni-SiC coatings deposited at 50 Hz showed the highest microhardness value (equal to 911.9 Hv).

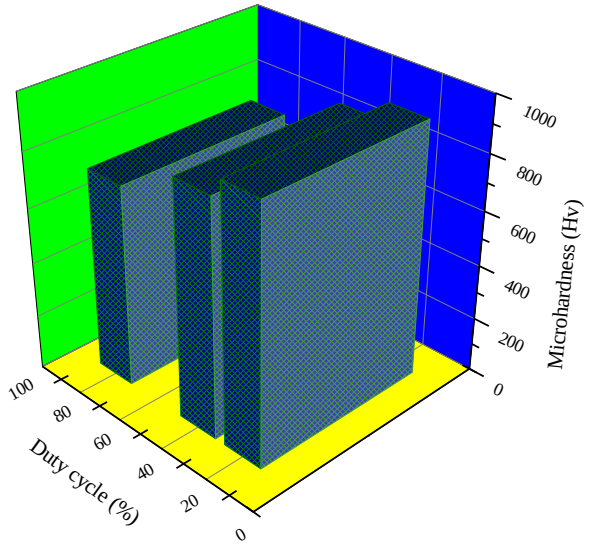

Figure 10. Effect of duty cycle on microhardnesses of Ni-SiC NCs prefabricated at 50 Hz pulse frequency.

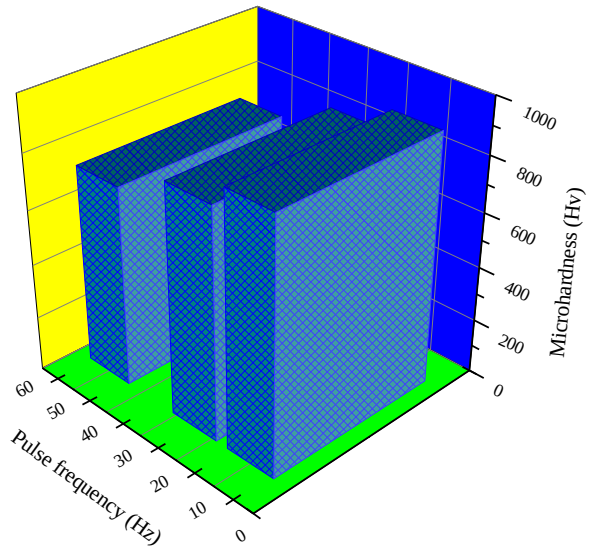

Figure 11. Effect of pulse frequency on microhardnesses of Ni-SiC NCs prefabricated at 20% duty

cycle.

Typically, NC microhardness depends on the hardness of the matrix and of the embedded ceramic particles [25, 26]. Therefore, coatings with high ceramic NP contents typically possess higher microhardness values. Ni-SiC NCs prepared at 50 Hz pulse frequency and 20% duty cycle contained the highest SiC contents, which explains their highest microhardness values.

3.5 Wear tests

The influence of the duty cycle and pulse frequency on the wear weight losses of the Ni-SiC NCs is displayed in Figs. 12 and 13, respectively.

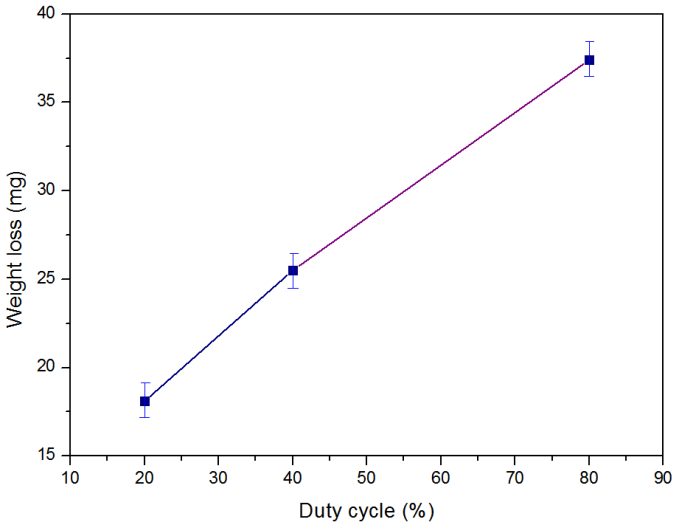

Figure 12. Effect of duty cycle on weight losses of Ni-SiC NCs prefabricated at 50 Hz pulse frequency.

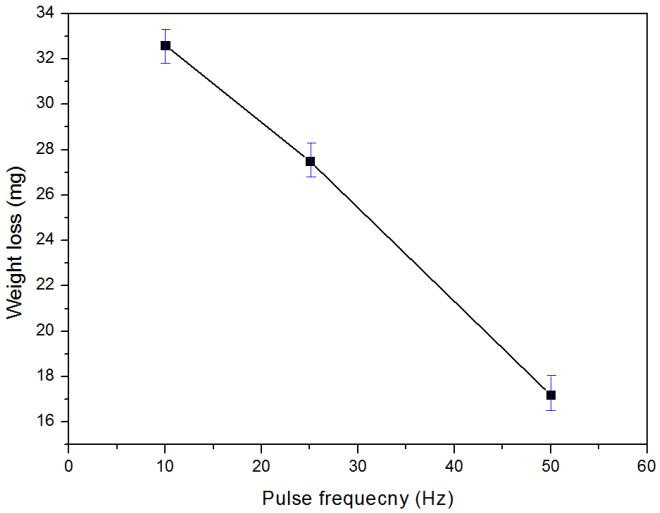

Figure 13. Effect of pulse frequency on weight losses of Ni-SiC NCs prefabricated at 20% duty cycle.

The wear weight losses of the Ni-SiC NCs (deposited at 50 Hz pulse frequency) decreased as

the duty cycle value decreased (see Fig. 12). The maximum wear weight loss (equal to 37.4 mg) was observed for the Ni-SiC NCs deposited at the 80% duty cycle. Wear weight loss of the Ni-SiC NC prepared at 20% duty cycle was only 18.1 mg, which indicates an excellent wear resistance.

The wear losses of the Ni-SiC NCs deposited at 20% duty cycle increased, as the pulse frequency was increased (see Fig. 13). The maximum wear loss (equal to 32.6 mg) was observed for the Ni-SiC NC obtained at 10 Hz. The minimum wear weight loss (equal to 17.2 mg) was observed for the Ni-SiC NC deposited at 50 Hz.

Thus, the coating deposited at 50 Hz pulse frequency and at 20% duty cycle showed the best wear resistance.

After the wear tests, surfaces of the Ni-SiC NCs deposited at 20% duty cycle (pulse frequency of 50 Hz) showed some minor abrasive grooves (see Fig. 14a). These grooves became more substantial and deeper as the duty cycle value was increased to 80% (see Figs. 14b-c). These results correlate very well with the wear weight loss data. The worst wear damages were observed for the Ni-SiC NCs deposited at 10 and 25 Hz (see Fig. 15). Ni-SiC NCs deposited at 50 Hz pulse frequency and at 20% duty cycle were the smoothest after the wear tests and showed only some minor scratches.

Accordingly, the wear reasons of Ni-SiC NCs can be linked to two aspects. Firstly, wear resistance of our Ni-SiC NCs was influenced by the SiC amount in the coating [27], because SiC incorporation into the composites with the metal matrices was expected to yield wear-resistant and very hard materials [28]. Thus, Ni-SiC NCs deposited at 20% duty cycle and 50 Hz pulse frequency exhibited prominent wear resistances. Secondly, higher contents of SiC NPs embedded in the NCs led to abruption of large number of SiC NPs from the nickel matrixes, forming great quantities of rolling grains during wear testing. This result could effectually hinder the growth of abrasive grooves, bringing about excellent wear resistance.

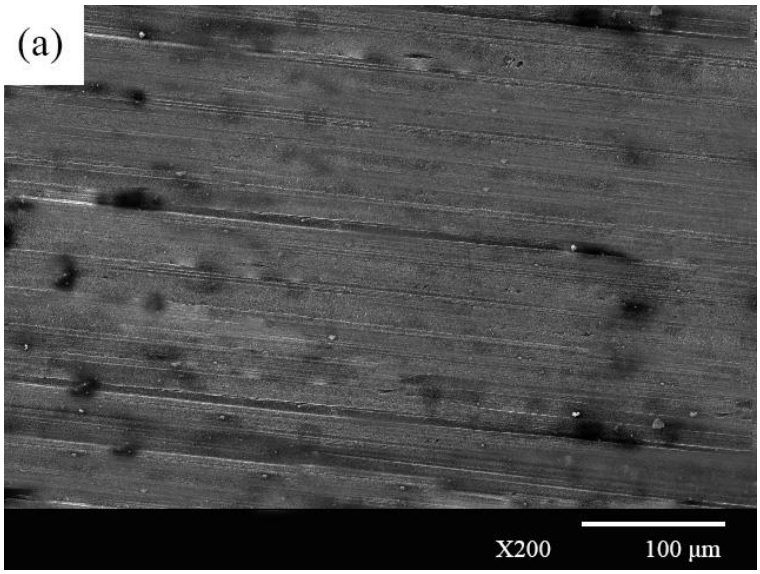

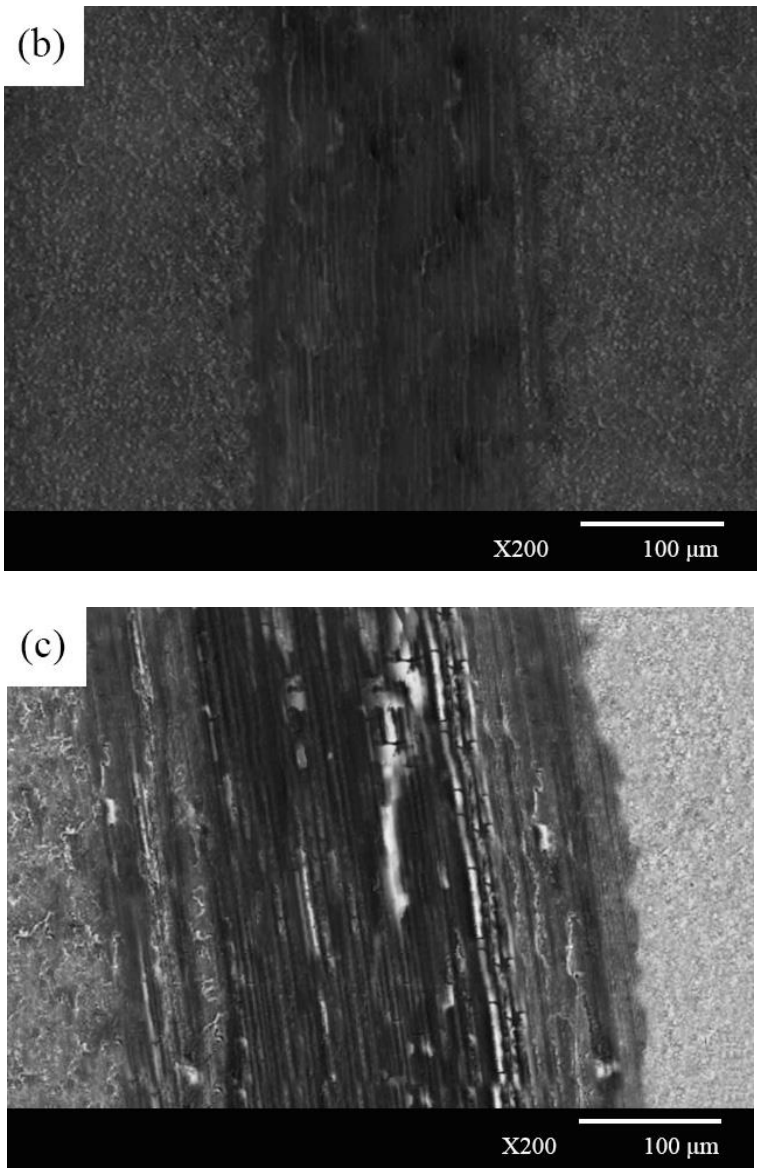

Figure 14. SEM images of the worn surface of Ni-SiC NCs prefabricated with different duty cycles: (a) 20%, (b) 40%, and (c) 80%.

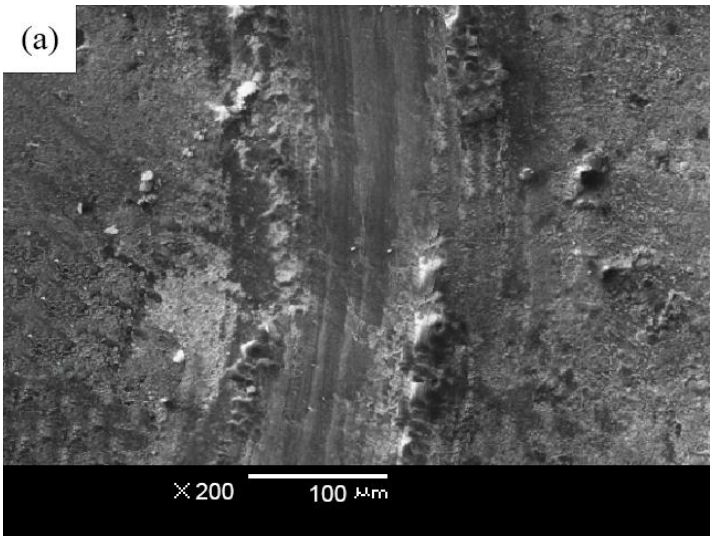

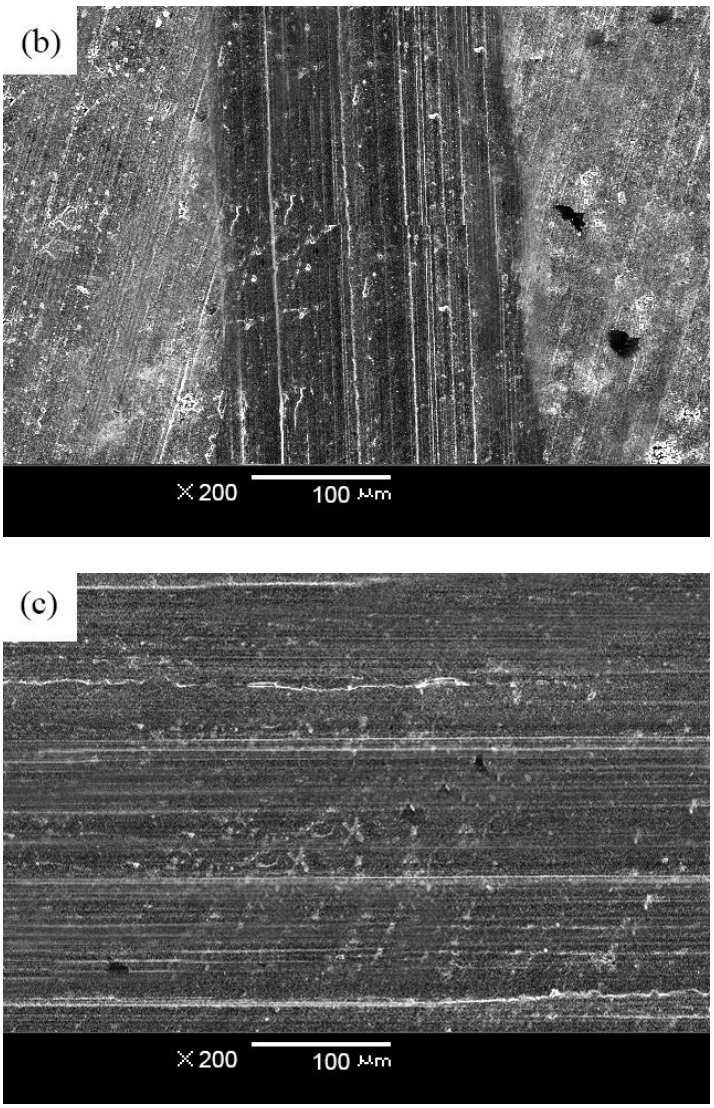

Figure 15. SEM images of the worn surface of Ni-SiC NCs prefabricated with different pulse frequencies: (a) 10 Hz, (b) 25 Hz, and (c) 50 Hz.

3.6 Corrosion tests

Figs. 16 and 17 reveal the Nyquist and Bode diagrams of Ni-SiC NCs prefabricated at different duty cycles and pulse frequencies, respectively. Table 3 depicts the charge-transfer resistance (R_{ct}) from the measured EIS diagrams on Ni-SiC NCs. Apparently, as the duty cycle decreased, the R_{ct} value increased, illustrating the increase in the corrosion resistance of Ni-SiC NCs. Moreover, with the increase in pulse frequency, the R_{ct} value also increased, demonstrating the increasing corrosion resistance. EIS of our Ni-SiC NCs deposited at 50 Hz pulse frequency and 20% duty cycle showed the highest impedance, which implies the best corrosion resistance. Composites prepared at other duty cycle and pulse frequency values showed lower impedance (thus, lower corrosion resistance) values. Our results are in agreement with those reported by Yang *et al.* [29], Jin *et al.* [30] and Singh *et al.* [31].

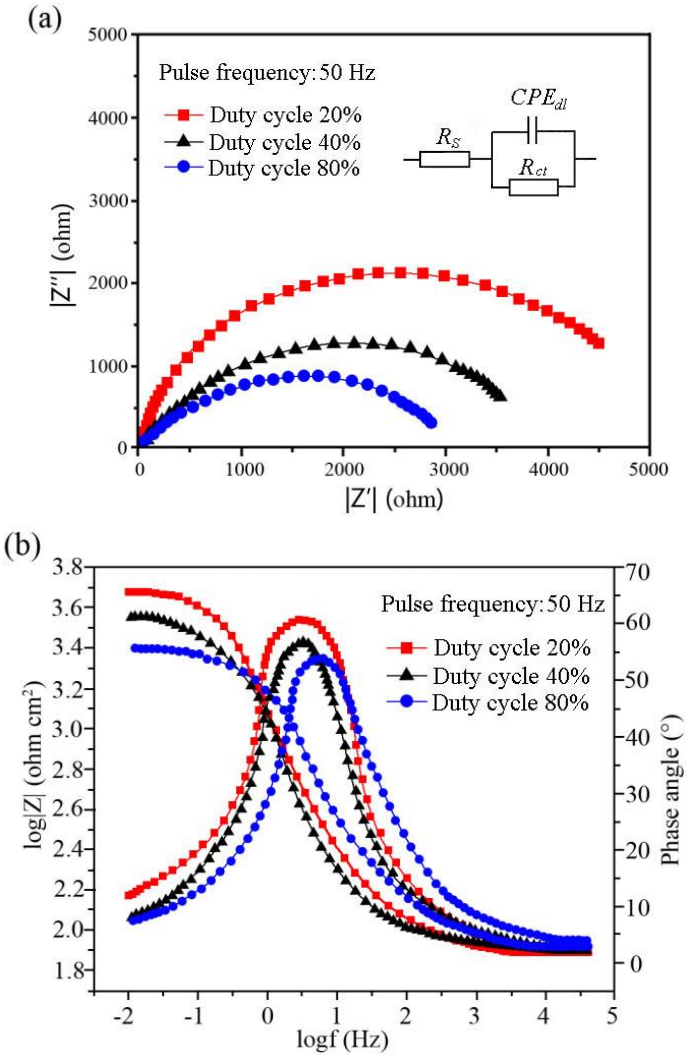

Figure 16. Nyquist (a) and Bode (b) diagrams measured on Ni-SiC NCs prefabricated at different duty cycles.

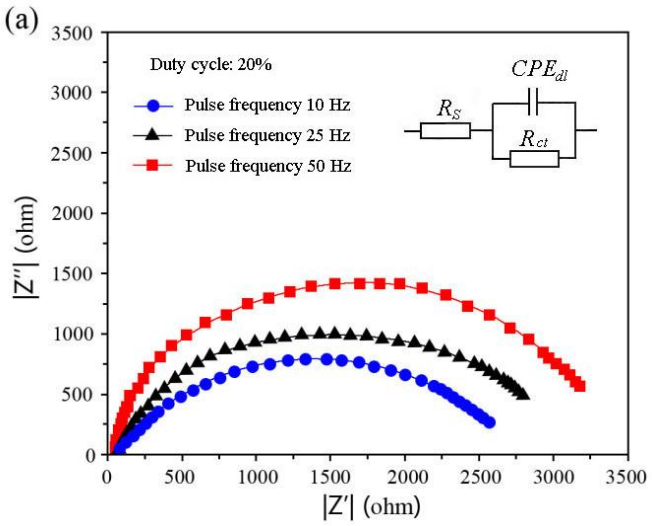

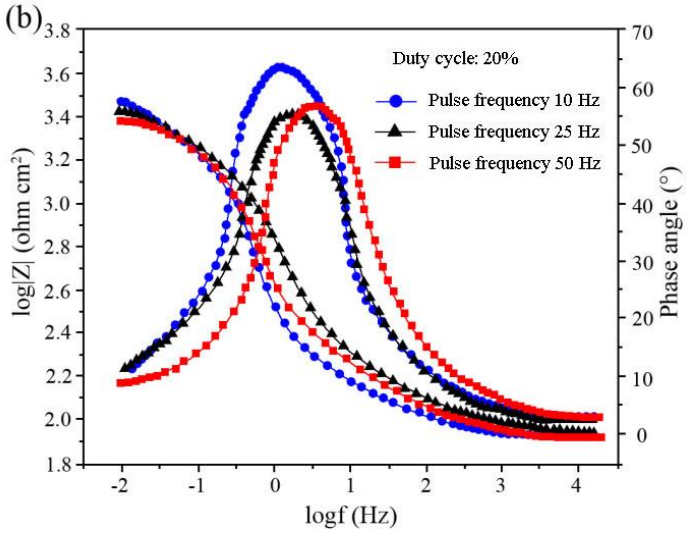

Figure 17. Nyquist (a) and Bode (b) diagrams measured on Ni-SiC NCs prefabricated at different pulse frequencies.

Table 3. Fitting of charge-transfer resistance from the measured EIS diagrams on Ni-SiC NCs fabricated under various duty cycles and frequencies.

		Charge-transfer resistance ($\Omega \cdot cm^2$)
Duty cycle (%)	20	5372.3
	40	3895.6
	80	3107.1
Pulse frequency (Hz)	10	2726.4
	25	3178.5
	50	3491.8

Therefore, fabrication of the Ni-SiC composites using optimized PCED plating parameters (such as pulse frequency and duty cycle values) resulted in the formation of the microstructurally uniform and fine-grained coatings. Such coatings would be capable of minimizing NaCl penetration the bulk of a Ni-SiC coating, preventing its corrosion. If the same coatings are fabricated with not thoroughly optimized parameters, the resulting Ni-SiC NC coating morphology would contain coarse, uneven, and loose grains. Such a coating would be very susceptible to the NaCl penetration and consequent corrosion.

4. CONCLUSION

(1) The duty cycle and pulse frequency significantly affected the surface morphologies of Ni-SiC NCs. The surface of the Ni-SiC NC obtained at the 20% duty cycle contained small Ni grains with smooth, uniform, and fine microstructure. When the coatings were prepared in the 25-50 Hz pulse

frequency range, SiC NPs were homogeneously dispersed in the coating, and the resulting NCs were uniform, compact and contained fine grains.

(2) TEM of the cross-section of the Ni-SiC sample deposited at 20% duty cycle, and 50 Hz pulse frequency showed abundant and homogeneously distributed SiC NPs in the Ni grains. In addition, duty cycle and pulse frequency values also affected SiC NP content.

(3) Ni peaks decreased and became broader as the pulse frequency was increased, and duty cycle value was decreased. Among NCs fabricated at different pulse frequencies and 20% duty cycle, Ni-SiC coatings deposited at 50 Hz showed the highest microhardness value (equal to 911.9 Hv).

(4) The wear weight losses of the Ni-SiC NCs (deposited at 50 Hz pulse frequency) decreased as the duty cycle value decreased. Wear weight loss of the Ni-SiC NC prepared at 20% duty cycle was only 18.1 mg, which indicates an excellent wear resistance. In addition, EIS of our Ni-SiC NCs deposited at 50 Hz pulse frequency and 20% duty cycle showed the highest impedance, which implies the best corrosion resistance.

ACKNOWLEDGEMENT
This work has been supported by the National Natural Science Foundation of China (Grant no. 51974089) and Natural Science Foundation of Heilongjiang Province of China (Grant no. LC2018020).

References

1. Z. Zhang and Q. Du, *J. Funct. Mater.,* 50(3) (2019) 3081. (In Chinese)
2. C. Ma, W. Yu, M. Jiang, W. Cui and F. Xia, *Ceram. Int.,* 44(5) (2018) 5163.
3. S. Tamariz, D. Martin and N. Grandjean, *J. Cryst. Growth,* 476 (2017) 58.
4. Q.L. Sun, J.L. Liu, H. Cheng, Y. Mou, J.X. Liu, Y. Peng and M.X. Chen, *Ceram. Int.,* 45 (2019) 18972.
5. Y. Xu, S. Ma, M. Fan, Y. Chen, X. Song and J. Hao, *Surf. Coat. Technol.* 363 (2019) 51.
6. P. Jin, C. Sun, C. Zhou and L. Shi, *Ceram. Int.,* 45(16) (2019) 20155.
7. C. Wang, L. Shen, M. Qiu, Z. Tian and W. Jiang, *J. Alloy. Compd.,* 727 (2017) 269.
8. F. Xia, W. Jia, C. Ma, R. Yang, Y. Wang and M. Potts, *Appl. Surf. Sci.,* 434 (2018) 228.
9. H. Zhou, W. Wang, Y. Gu, X. Fang and Y. Bai, *Strength Mater.,* 1 (2017) 1.
10. B. Li, W. Zhang, W. Zhang and Y. Huan, *J. Alloy. Compd.,* 702 (2017) 38.
11. M. Wu, W. Jia and P. Lv, *Procedia Eng.,* 174 (2017) 717.
12. B. Li, *Int. J. Electrochem. Sci.,* 12(8) (2017) 7017.
13. C.Y. Ma, D.Q. Zhao, F.F. Xia, H.Z. Xia, T. Williams and H.Y. Xing, *Ceram. Int.,* 46 (2020) 6115.
14. N.P. Wasekar, S. Madhavi Latha, M. Ramakrishna, D.S. Rao and G. Sundararajan, *Mater. Des.* 112 (2016) 140.
15. W. Liu, K. Jiang, M. Jiang and X. Li, *Ordnance Mater. Sci. Eng.,* 42(1) (2019) 17. (in Chinese)
16. R. Sen, S. Das and K. Das, *Surf. Coat. Tech.,* 205(13-14) (2011) 3847.
17. S. Jiang, S. Gao, J. Kong and X. Jin, *RSC Adv.,* 9(41) (2019) 23785.
18. Z. Szklarz, J. Lekki, P. Bobrowski, M.B. Szklarz and Ł. Rogal, *Mater. Chem. Phys.,* 215 (2018) 385.
19. S.K. Brantov, and E.B. Yakimov, *Semiconductors,* 53(2) (2019) 231.
20. F. Xia, W. Jia, C. Ma and J. Wang, *Ceram. Int.,* 44 (2018) 766.
21. B. Bahadormanesh, A. Dolati and M.R. Ahmadi, *J. Alloy. Compd.,* 509 (2011) 9406.

22. Y. Yang and Y.F. Cheng, *Surf. Coat. Tech.,* 205(10) (2011) 3198.
23. F. Xia, J. Tian, C. Ma, M. Potts and X. Guo, *J. Appl. Phys.,* 116 (2014) 234301.
24. M. Sajjadnejad, N. Setoudeh, A. Mozafari, A. Isazadeh and H. Omidvar, *Trans. Indian Inst. Met.* 70(6) (2017) 1533.
25. C. Ma, M. Jiang and F. Xia, *Surf. Rev. Lett.,* 24(5) (2016) 1750063.
26. F. Xia, Q. Li, C. Ma and X. Guo, *Ceram. Int.,* 46 (2) (2020) 2500.
27. K.H. Hou, M.D. Ger, L.M. Wang and S.T. Ke, *Wear,* 253 (2002) 994.
28. C. Sun, X. Liu, C. Zhou, C. Wang and H. Cao, *Ceram. Int.,* 45(1) (2019) 1348.
29. Y. Yang and Y.F. Cheng, *Surf. Coat. Tech.,* 216 (2013) 282.
30. P. Jin, C.F. Sun, Z.H. Zhang, C.Y. Zhou and T. Williams, *Surf. Coat. Tech.,* 392 (2020) 125738.
31. S. Singh, M. Sribalaji, N.P. Wasekar, S. Joshi, G. Sundararajan, R. Singh and A.K. Keshri, *Appl. Surf. Sci.,* 364(2016) 264.